Curcumin-mediated photodynamic inactivation of *Escherichia coli*, *Pseudomonas fluorescens*, and *Candida auris*

Jaime A. Garcia-Diosa,[a,1] Bhanu K. Pothineni,[a,2] and Adrian Keller[a,*]

[a] Paderborn University, Technical and Macromolecular Chemistry, Warburger Str. 100, 33098 Paderborn, Germany

***** Correspondence: adrian.keller@uni-paderborn.de

[1] present address: Martin-Luther-Universität Halle-Wittenberg, Institut für Pharmazeutische Technologie und Biopharmazie, Weinbergweg 22, D-06120 Halle (Saale), Germany

[2] present address: Programmable Biomaterials Laboratory, Institute of Materials, School of Engineering, École Polytechnique Fédérale de Lausanne, Lausanne 1015, Switzerland

Abstract

Photodynamic therapy (PDT) is an emerging antimicrobial strategy that uses light to activate photosensitizers, generating reactive oxygen species (ROS) that induce microbial cell death. This study investigates the antimicrobial efficacy of curcumin-mediated PDT against the microbial pathogens *Escherichia coli*, *Pseudomonas fluorescens*, and *Candida auris*. The minimum inhibitory concentration (MIC) for each microorganism is determined at different light fluence rates within a clinically relevant range. Our results demonstrate that curcumin-mediated PDT effectively inactivates *E. coli* and *C. auris*, while exhibiting only partial inhibition against *P. fluorescens* at curcumin concentrations up to 60 µM. Notably, within the tested fluence rate range, the total light dose appears to be a more critical determinant of antimicrobial efficacy than the specific fluence rate itself. The observed variations in microbial susceptibility highlight the importance of species-specific factors, such as cell wall/membrane structure. These findings provide guidelines for the application of curcumin-mediated PDT in combatting antimicrobial resistance.

Keywords: curcumin; photosensitizer; antimicrobial photodynamic therapy; bacteria; fungi

1. Introduction

The escalating challenge of antimicrobial resistance (AMR) calls for novel therapeutic strategies to combat infections caused by bacteria, fungi, viruses, and parasites (Laxminarayan et al. 2016). Traditional antibiotic treatments are becoming increasingly ineffective, posing a significant threat to global health. In this context, photodynamic therapy (PDT) has emerged as a promising therapeutic modality that utilizes light to activate photosensitizing agents, generating reactive oxygen species (ROS) that damage essential cellular components and ultimately cause the death of the microorganism (Dougherty et al. 1998; Ghorbani et al. 2018). PDT has demonstrated efficacy against a broad spectrum of microorganisms, including multidrug-resistant bacterial and fungal strains, positioning it as a valuable tool in combating AMR (Youf et al. 2021). Unlike conventional antibiotics, the multi-target mechanism of action of PDT reduces the likelihood of resistance development (Wainwright 1998; Youf et al. 2021). Resistance to antimicrobial PDT (aPDT) is rarely reported, suggesting that while the possibility of microbial adaptation and escape from this treatment may exists, it is currently limited (Cieplik et al. 2018). This is a crucial advantage in the face of rapidly evolving resistance mechanisms in pathogenic bacteria and fungi.

Despite its advantages, aPDT faces a number of challenges that impede its widespread clinical adoption. Common photosensitizers (PSs) often suffer from issues such as limited tissue penetration, lack of selectivity, aggregation and quenching, and dark toxicity, resulting in intense research efforts dedicated to the development and discovery of new PSs (Klausen et al. 2020; Polat and Kang 2021; Huis In 't Veld et al. 2023). Curcumin, a naturally occurring polyphenol derived from turmeric (*Curcuma longa*), has emerged as a promising alternative due to several key advantages. These include high biocompatibility, low systemic toxicity, and synergistic therapeutic effects, such as anti-proliferative, anti-inflammatory, and anti-angiogenic activities (Dias et al. 2020). Consequently, it is investigated in various implementations of PDT, most importantly in cancer therapy (Xie et al. 2022) but also in the treatment of oral infections (Santezi et al. 2018). Furthermore, since curcumin is a common food ingredient and food additive, it is frequently used in the photodynamic inactivation of foodborne pathogens in various food products (Yu et al. 2022; Lan et al. 2023).

The PDT effect depends on the interaction of three essential components: molecular oxygen, the PS, and light. The PDT dose can be controlled by adjusting the latter two components. It is generally assumed that the biological effect of light in PDT is determined by the total light dose, regardless of the exposure time (Gao et al. 2020). Consequently, PDT studies often present data in terms of total light dose to compare the photoinactivation of microorganisms (Dias et al. 2020; Jao et al. 2023; Law et al. 2023). However, the fluence rate, *i.e.*, the power density of light, may influence PDT efficacy by affecting metabolic oxygen consumption and, consequently, the efficiency of ROS production (Nichols and Foster 1994; Henderson et al.

68 2006; Ghorbani et al. 2018). Indeed, some studies on the photodynamic treatment of cancer
69 cells and tumors have shown that lower fluence rates can enhance the cytotoxic effect of the
70 treatment by optimizing the depletion of the cell's antioxidant defenses (Angell-Petersen et
71 al. 2006; Yamamoto et al. 2006; Wang et al. 2007; Woodhams et al. 2007; Grossman et al.
72 2016; Dos Santos et al. 2020). However, there are only few reports on this phenomenon in
73 aPDT. Qin *et al.* conducted a study on the effect of different parameters of toluidine blue-
74 mediated PDT effectiveness, including fluence rate, on the inactivation of periodontal
75 pathogens. They observed that a high fluence rate (159 mW cm^{-2}) increases the cytotoxicity
76 of the treatment (Qin et al. 2008). A similar conclusion was reported by Prates *et al.*, who
77 studied the effects of fluence rate and light dose on the treatment of three different strains
78 of *Candida sp.* using methylene blue as the PS. In these experiments, a higher fluence rate
79 (300 mW cm^{-2}) lead to a higher cytotoxicity of the treatment, although the production of ROS
80 is inversely proportional to the fluence rate (Prates et al. 2009). Due to the limited number of
81 studies, the role of the fluence rate in aPDT is not fully understood. Additionally, these studies
82 used fluence rates that are much higher than those recommended to avoid possible damage
83 to host tissue in clinical applications (Sitnik and Henderson 1998; Jori et al. 2006).

84 In this study, we evaluate the efficacy of curcumin-mediated photodynamic inactivation of
85 three relevant pathogens by determining their minimum inhibitory concentrations (MICs) at
86 different fluence rates within a clinically relevant range. It has been observed before that
87 different bacterial species show markedly different susceptibilities to curcumin-mediated
88 photodynamic inactivation (Penha et al. 2017), which have to be considered in the
89 development of effective treatment protocols. For the current investigation, we have
90 selected *Escherichia coli*, *Pseudomonas fluorescens*, and *Candida auris* as the target
91 pathogens. *E. coli* is a Gram-negative bacterium that causes a wide range of infections
92 (Nataro and Kaper 1998; Rangel et al. 2005) and thus is a frequent target of aPDT. *P.*
93 *fluorescens* is a common food contaminant capable of growing at a wide range of
94 temperatures, making it a significant issue in both refrigerated and unrefrigerated food items
95 (Kumar et al. 2019). Curcumin-mediated inactivation of *P. fluorescens*, therefore, has been
96 investigated almost exclusively in food items (Saraiva et al. 2021; Saraiva et al. 2024; Zheng
97 et al. 2025). However, *P. fluorescens* can also cause severe infections in
98 immunocompromised individuals, most importantly bacteremia due to contaminated
99 medical equipment (Gershman et al. 2008), but also skin and soft tissue infections, as well
100 as respiratory tract infections (Liu et al. 2021), which warrants investigations also in the
101 context of aPDT settings. *C. auris* is a newly emerged fungal pathogen that has become a
102 global threat due to its rapid spread and multidrug resistance (Du et al. 2020). Photodynamic
103 inactivation of *C. auris* has already been demonstrated using several PSs (Bapat and Nobile
104 2021; Grizante Barião et al. 2022; Silva et al. 2023), but not with curcumin. By investigating
105 the combined effects of curcumin concentration and fluence rate on these target pathogens,

this study aims to contribute to a better understanding of the factors influencing the efficacy of curcumin-mediated aPDT and its potential as a novel antimicrobial strategy to combat the growing challenge of antimicrobial resistance.

2. Results and discussion

Figure 1 evaluates *E. coli* growth after 420 nm irradiation with a fluence rate of 17.8 mW cm^{-2} and 76.3 mW cm^{-2}, respectively. The control samples incubated in the dark exhibit a relatively stable ΔOD_{600} value of approximately 0.4, indicative of normal bacterial growth and no dark cytotoxicity (see Figure 1A). In contrast, the samples irradiated at 420 nm with both fluence rates (17.8 mW cm^{-2} and 76.3 mW cm^{-2}) demonstrate a sharp decline from ΔOD_{600} values of 0.4 to almost zero at curcumin concentrations of 7.5 µM and above (see Figure 1A). Notably, no significant difference in bacterial growth inhibition is observed between the two fluence rates. This suggests that the maximum aPDT effect is reached once the curcumin concentration is 7.5 µM or above, regardless of the fluence rate within the therapeutic window. The images of *E. coli* cultures on agar plates after 24 h of aPDT provide a visual confirmation of the quantitative ΔOD_{600} data (see Figure 1B and Figure S1). The control plates (black outline) show confluent bacteria at the maximum curcumin concentration investigated, consistent with the ΔOD_{600} values. After aPDT, plates corresponding to curcumin concentrations of 1.88 µM and 7.5 µM (blue and red outlines) show a clear reduction in colony forming units compared to the control, consistent with the ΔOD_{600} measurements.

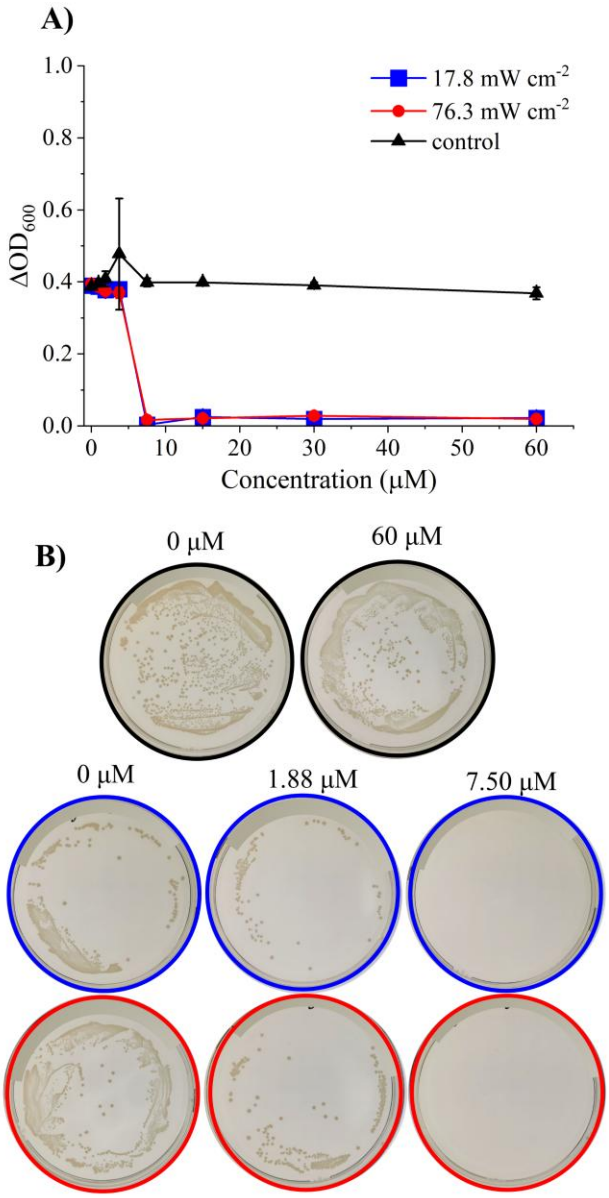

Figure 1. *E. coli* growth after curcumin-mediated aPDT using 420 nm light at a dose of 20 J cm^{-2} with fluence rate of 17.8 mW cm^{-2} and 76.3 mW cm^{-2}, respectively, at different curcumin concentrations. A) Optical density change (ΔOD_{600}) after 24 h of incubation at 37 °C. Error bars indicate the standard deviation (n = 3). Controls were incubated in the dark. B) *E. coli* cultures (24 h) on agar after aPDT at different curcumin concentrations and fluence rates. Control (incubated in the dark, black outline), low fluence rate (blue outline), and high fluence rate (red outline).

Figure 2 presents the results of curcumin-mediated aPDT on *P. fluorescens* with both fluence rates at different curcumin concentrations. Again, the control samples exhibit a stable

139 ΔOD_{600} value, indicating consistent bacterial growth and no dark cytotoxicity. In contrast,
140 samples treated with aPDT demonstrate a concentration-dependent decrease of ΔOD_{600}
141 values, indicative of a reduction of bacterial viability (see Figure 2A). At the lower fluence rate
142 (17.8 mW cm^{-2}), a remarkable linear decrease of ΔOD_{600} is observed at curcumin
143 concentration higher than 15 µM. Similarly, at the highest fluence rate (76.3 mW cm^{-2}), ΔOD_{600}
144 values decrease with increasing curcumin concentration. However, this decrease starts
145 already at the lowest curcumin concentration investigated and appears to saturate for the
146 highest concentrations. Bacterial growth is detected even at 60 µM curcumin. This is
147 consistent with the *P. fluorescens* cultures on agar plates shown in Figure 2B and Figure S2.
148 Samples treated with PDT at 15 µM and 60 µM curcumin at both fluence rates (blue and red
149 outlines), show a clear reduction in colony forming units compared to the control, but no
150 complete bacterial inhibition is observed.

151

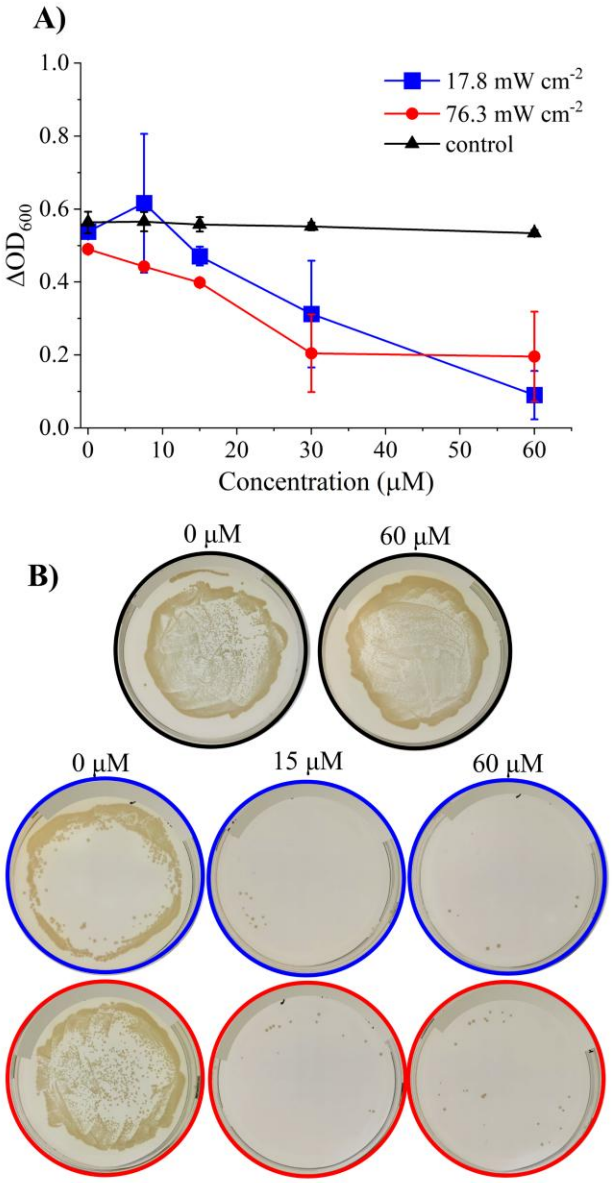

Figure 2. *P. fluorescens* growth after curcumin-mediated aPDT using 420 nm light at a dose of 20 J cm^{-2} with fluence rate of 17.8 mW cm^{-2} and 76.3 mW cm^{-2}, respectively, at different curcumin concentrations. A) Optical density change (ΔOD_{600}) after 24 h of incubation at 30 °C. Error bars indicate the standard deviation (n = 3). Controls were incubated in the dark. B) *P. fluorescens* cultures (48 h) on agar after aPDT at different curcumin concentrations and fluence rates. Control (incubated in the dark, black outline), low fluence rate (blue outline), and high fluence rate (red outline).

The results of curcumin-mediated aPDT on *C. auris* at low and high fluence rates are shown in Figure 3. The control samples exhibit a relatively stable ΔOD_{600} value around 0.65 – 0.70

across varying curcumin concentrations, showing consistent growth of the yeast and no dark cytotoxicity (see Figure 3A). On the other hand, irradiated samples show a markedly concentration-dependent decrease in ΔOD_{600} values. At both fluence rates (17.8 mW cm^{-2} and 76.3 mW cm^{-2}), a strong reduction of the fungal growth is observed even at the lowest curcumin concentration used (1.87 μM). When the curcumin concentration reaches 15 μM and more, the ΔOD_{600} values approaches zero, indicating a near-complete inhibition of fungal growth (see Figure 3A). Notably, there is again no significant difference between the two fluence rates at any of the tested curcumin concentrations. This suggests that within the tested fluence range, the curcumin concentration is the primary parameter of the photodynamic effect. *C. auris* cultures on agar plates after aPDT visually confirm the trends observed in the ΔOD_{600} measurements (see Figure 3B and Figure S3). The control group shows dense *C. auris* growth, consistent with the high ΔOD_{600} values. In the case of the samples irradiated at both fluence rates (blue and red outlines), a strong reduction in the number of colonies is observed at 3.75 μM, whereas at 15 μM, visible colonies are almost complete absent (see Figure 3B and Figure S3), corroborating the trend of the ΔOD_{600} values.

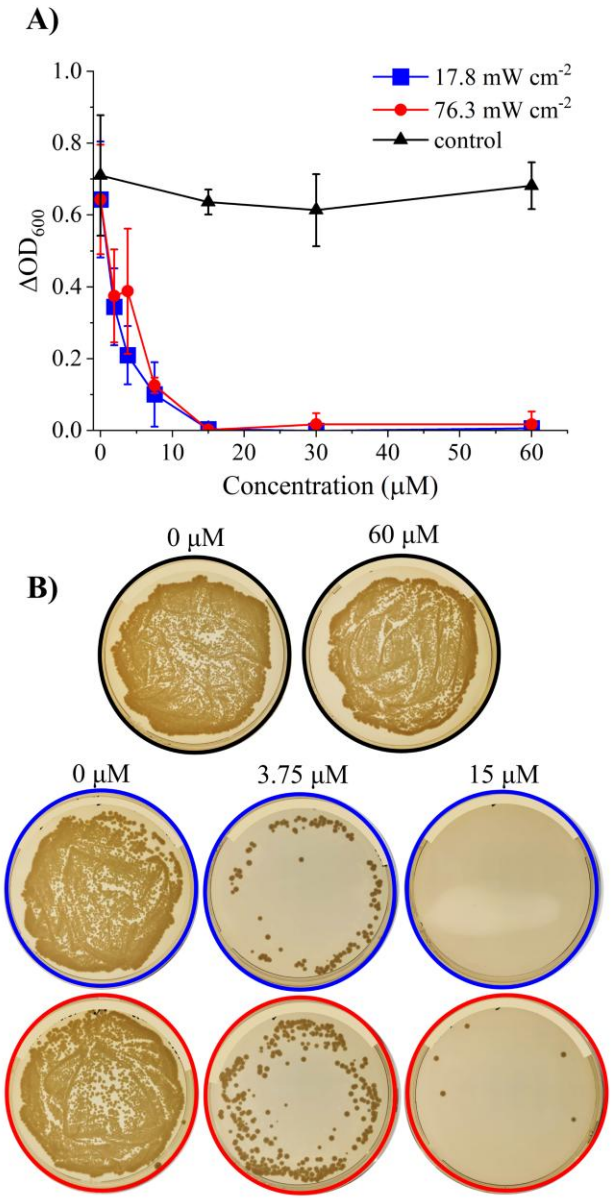

Figure 3. *C. auris* growth after curcumin-mediated aPDT using 420 nm light at a dose of 20 J cm^{-2} using with fluence rate of 17.8 mW cm^{-2} and 76.3 mW cm^{-2}, respectively, at different curcumin concentrations. A) Optical density change (ΔOD_{600}) after 24 h of incubation at 37 °C. Error bars indicate the standard deviation (n = 3). Controls were incubated in the dark. B) *C. auris* cultures (24 h) on agar after aPDT at different curcumin concentrations and fluence rates. Control (incubated in the dark, black outline), low fluence rate (blue outline), and high fluence rate (red outline).

Table 1 summarizes the MIC of curcumin during aPDT for *E. coli*, *P. fluorescens*, and *C. auris* as determined from the OD_{600} results. The data reveal a remarkable difference in the

susceptibility of the three microorganisms to curcumin-mediated aPDT. *E. coli* exhibits the highest sensitivity of the treatment, with a MIC of 7.5 μM, implying that a relatively low concentration of curcumin is sufficient to inhibit *E. coli* growth. *C. auris* demonstrates intermediate susceptibility with a MIC of 15 μM, requiring a higher curcumin concentration to effectively inhibit the growth of the yeast. On the other hand, *P. fluorescens* shows the lowest susceptibility to curcumin-mediated aPDT with a MIC greater than 60 μM, indicating that *P. fluorescens* is significantly more resistant to the photodynamic effects of the PS curcumin under the studied conditions.

Table 1. Minimum inhibitory concentrations (MICs) of curcumin during aPDT using a fluence rate range of 17.8 – 76.3 mW cm^{-2}, and a total light dose of 20 J cm^{-2}.

Microorganism	**MIC (μM)**
E. coli	7.5
P. fluorescens	> 60.0
C. auris	15.0

Our results demonstrate that curcumin-mediated aPDT is effective in inactivating *E. coli* and *C. auris*, and partially inactivating *P. fluorescens* at curcumin concentrations up to 60 μM. These results are consistent with previous studies, which have reported varying degrees of susceptibility to curcumin-mediated aPDT among different microorganisms (Dovigo, Pavarina and Ribeiro et al. 2011; Andrade et al. 2013; Penha et al. 2017; Saraiva et al. 2021; Saraiva et al. 2024). For instance, *P. fluorescens* has been shown to be more resistant to curcumin-mediated aPDT compared to *E. coli* and *C. albicans* (Saraiva et al. 2021; Saraiva et al. 2024). This difference in susceptibility may be attributed to several factors, including variations in cell wall/membrane structure and composition, and variations in the uptake and intracellular accumulation of curcumin among the different microorganisms. In general, curcumin can interact with microorganisms through several mechanisms, including charge interactions, which are pH-dependent due to keto-enol tautomerism (Priyadarsini 2009), binding to various enzymes such as sortase A (Hu et al. 2013; Praditya et al. 2019) and FtsZ (Kaur et al. 2010), and membrane adsorption and subsequent uptake into the cell. Species-specific differences may play a role in all these mechanisms but are particularly important for cellular uptake (Annunzio et al. 2018).

This study highlights the importance of species-specific variations in susceptibility to curcumin-mediated aPDT. Despite sharing a common Gram-negative cell wall structure with

219 an outer membrane containing lipopolysaccharides (LPSs), *E. coli* and *P. fluorescens* display
220 markedly different responses to aPDT with curcumin (see Table 1). While the precise
221 mechanisms governing the interaction of curcumin with these species remain to be fully
222 elucidated, the high efficacy of curcumin-mediated aPDT against *E. coli* suggests that
223 curcumin can effectively penetrate the outer membrane, likely via charge-mediated
224 interactions, leading to subsequent membrane disruption by the generated ROS (Oliveira et
225 al. 2018; Gao et al. 2019). In contrast, the significantly elevated MIC for *P. fluorescens*
226 suggests a potential limitation in curcumin accumulation within the cell, probably due to
227 reduced uptake or increased efflux mechanisms.

228 In the case of *C. auris*, a cell wall composed of chitin, glucans, and mannans is present,
229 which differs significantly from bacterial cell walls (Free 2013). However, the intermediate
230 susceptibility to curcumin-mediated aPDT compared to *E. coli* and *P. fluorescens* (see Table
231 1), suggests that curcumin can effectively penetrate the *C. auris* cell wall and accumulate
232 within the cell at a higher rate than for *P. fluorescens*. This is in line with previous observations
233 of effective curcumin-mediated photodynamic inactivation of various *Candida* species
234 (Dovigo, Pavarina and Carmello et al. 2011; Dovigo, Pavarina and Ribeiro et al. 2011; Andrade
235 et al. 2013). The observed variations in susceptibility among the different microorganisms
236 underscore the importance of considering species-specific factors, such as cell
237 wall/membrane structure, and curcumin uptake mechanisms, when evaluating the
238 effectiveness of aPDT.

239 Regarding the fluence rate effect on the PDT efficiency, several studies in cancer treatment
240 suggest that lower fluence rates at the same total light dose with a longer treatment time can
241 be more efficient in PDT compared to higher fluence rates (Henderson et al. 2006; Dos
242 Santos et al. 2020; Gao et al. 2020). The reasons behind this effect of the fluence rate are still
243 under investigation, but some studies suggest that oxygen availability plays an important
244 role. Lower fluence rates would allow for more efficient oxygen diffusion into the target tissue,
245 whereas high fluence rates lead to the depletion of available oxygen, thereby limiting ROS
246 generation and ultimately reducing PDT efficacy (Dougherty et al. 1998; Alvarez and Sevilla
247 2024). Conversely, some reports suggest an inverse relationship between fluence rate and
248 aPDT efficiency (Qin et al. 2008; Prates et al. 2009). While higher fluence rates may lead to
249 increased PS bleaching, they have also been associated with greater microbial inhibition
250 (Prates et al. 2009). This apparent contradiction may be explained by a potential initial surge
251 in ROS formation at higher fluence rates, followed by photobleaching. However, increasing
252 the fluence rate infinitely to enhance aPDT efficacy is not feasible. Photon absorption by the
253 PS is limited, restricting ROS production, and the photobleaching effect becomes
254 increasingly significant (Qin et al. 2008). Furthermore, to minimize host tissue damage, the

255 therapeutic window for aPDT is generally considered to be below approximately 50 mW cm^{-2}
256 (Jori et al. 2006).

257 In this study, the tested fluence rates (17.8 – 76.3 mW cm^{-2}) did not significantly influence the
258 antimicrobial activity within the tested concentration range. This finding suggests that the
259 moderate changes of the fluence rate possible within the therapeutic window are insufficient
260 to induce significant variations in ROS generation. Under these conditions, the total light
261 dose thus appears to be the primary determinant of aPDT efficacy. Nevertheless, future
262 studies should investigate a wider range of fluence rates and total light doses to further
263 elucidate the impact of these parameters on aPDT efficacy. Furthermore, investigating the
264 underlying mechanisms of curcumin-mediated aPDT in these and other microorganisms,
265 including the role of specific cellular targets and the generation of ROS, will provide valuable
266 insights for optimizing this approach and developing novel antimicrobial strategies.

267

268 **3. Experimental**

269 *3.1. Bacteria culture*

270 *E. coli* W1485 (DSM 5695) and *P. fluorescens* 1175 (DMS 1976) were purchased from Leibniz
271 Institute DSMZ. For bacteria culture preparation, two or three bacterial colonies were
272 suspended in 30 mL LB medium (MP Biomedicals) and incubated overnight at 37 °C for *E.*
273 *coli* or 24 h at 30 °C for *P. fluorescens*. In the case of *E. coli*, 250 µL overnight suspension was
274 used to inoculate fresh LB medium and incubated for 4-6 h at 37 °C. For *P. fluorescens*, the
275 culture incubated for 24 h was used directly. Lastly, the bacteria suspensions were
276 centrifuged, washed, and resuspended in 5 % dimethyl sulfoxide (DMSO, Carl Roth),
277 adjusting the optical density at 600 nm (OD_{600}) to 0.2. DMSO was used as a solvent to ensure
278 the solubility of curcumin (Saraiva et al. 2021). At a concentration of 5 %, DMSO has been
279 reported to exert minimal cytotoxic effects on bacteria (Ansel et al. 1969; Tunçer Çağlayan
280 and Gurbanov 2024).

281 *3.2. Fungi culture*

282 *C. auris* (DSM 105990) was purchased from Leibniz Institute DSMZ. The fungi culture was
283 prepared using two or three colonies, which were resuspended in 30 mL yeast extract
284 peptone dextrose medium (YPD medium, SERVA) and incubated at 180 rpm and 37 °C
285 overnight. Finally, the culture was centrifuged, washed, and resuspended in 5 % dimethyl
286 sulfoxide (DMSO), adjusting the optical density (OD_{600}) to 0.2.

287 *3.3. Antimicrobial photodynamic inactivation*

288 Photodynamic inactivation was performed using a Lumidox II 96-position LED array 420 nm
289 with cooling base (Analytical Sales and Services) with Curcumin (Sigma Aldrich) as the PS.
290 The experiments were performed in triplicate using the microdilution method in sterile 96-
291 wells microplates. 50 µL aliquots of microbial suspension in 5 % DMSO (OD_{600} = 0.2) were
292 added to 50 µL of curcumin in 5 % DMSO. The microplates were incubated for 30 min at 25 °C
293 before photodynamic inactivation. Control samples without curcumin and light irradiation
294 were also prepared to analyze the curcumin toxicity and light-induced inhibition.

295 The fluence rate effect in the photodynamic inactivation was evaluated at a constant light
296 dose of 20 J cm^{-2} using the lowest and highest fluence rate levels available in the Lumidox II
297 equipment. Since the 96-well microplate was held at 17 mm from the light source, the
298 samples were irradiated for 1123 s at the lowest fluence rate (17.8 mW cm^{-2}), and for 262 s at
299 highest fluence rate (76.3 mW cm^{-2}), obtaining a light dose of 20 J cm^{-2} at both fluence rates.
300 At these short exposure times, the potential impact of prolonged DMSO exposure on
301 bacterial growth is minimized. For subsequent minimum inhibitory concentration (MIC)
302 assays, the DMSO concentration was reduced to 1%, a level generally considered to have
303 negligible or no effect on bacterial viability (Ansel et al. 1969; Liu et al. 2023). Furthermore,
304 all photodynamic inactivation experiments were conducted in the absence of bacterial
305 growth media to prevent light absorption by medium components, and to minimize
306 interactions with ROS, which could ultimately reduce the effectiveness of PDT.

307 *3.4. Optical density measurements*

308 Photodynamic inactivation at the different fluence rates was studied by measuring the
309 change in the OD_{600} (ΔOD_{600}) of the treated samples after 24 h of incubation in their respective
310 media. After treatment, a 20 µL aliquot of each sample was added to 80 µL (1 % DMSO final
311 concentration) of LB (*E. coli and P. fluorescens*) or YPD medium (*C. auris*), in sterile 96-well
312 microplates. Then, the microplates were incubated at 37 °C (*E. coli* and *C. auris*) or at 30 °C
313 (*P. fluorescens*). The OD_{600} values were measured at the beginning and after 24 h of
314 incubation using a microplate reader TrisStar^2 S LB 942 (Berthold technologies). The ΔOD_{600}
315 value is an indicator of the growth or inhibition of microbes.

316 *3.5. Agar plate culture*

317 For visual inspection of photodynamic inactivation, 80 µL aliquots of treated samples were
318 spread on agar plates and incubated. *E. coli* was incubated on LB agar plates at 37 °C for 24
319 h. *P. fluorescens* was incubated on LB agar plates at 30 °C for 48 h. *C. auris* was incubated
320 on YPD agar plates at 37 °C for 24 h.

321 *3.6. Statistical analysis*

322 The change in optical density at 600 nm (ΔOD_{600}) was measured in triplicate for each
323 experimental condition (n = 3). Data are presented as mean ± standard deviation (SD) of the
324 three values.

325

326 **4. Conclusions**

327 This study investigated the antimicrobial efficacy of curcumin-mediated aPDT against *E. coli*,
328 *P. fluorescens*, and *C. auris* using a range of curcumin concentrations and two distinct
329 fluence rates. Our findings demonstrate that curcumin-mediated aPDT is able to effectively
330 inactivate *E. coli* and *C. auris*, while leading only to partial inhibition of *P. fluorescens* at
331 curcumin concentrations up to 60 µM. Notably, within the tested fluence rate range (17.8 –
332 76.3 mW cm^{-2}), no significant difference in antimicrobial activity was observed, suggesting
333 that within the therapeutic window, the total light dose is a more critical determinant of aPDT
334 efficacy than the specific fluence rate itself.

335 The observed variations in microbial susceptibility to curcumin-mediated aPDT highlight the
336 importance of species-specific factors, such as cell wall/membrane structure, and
337 curcumin uptake and accumulation. While the mechanisms responsible for the observed
338 differences remain to be fully elucidated, our results suggest that curcumin effectively
339 penetrates the bacterial cell wall of *E. coli* and the fungal cell wall of *C. auris*, leading to
340 significant growth inhibition. In contrast, the limited efficacy against *P. fluorescens* may be
341 attributed to reduced curcumin uptake or increased efflux mechanisms.

342 These findings provide valuable insights into the potential of curcumin-mediated aPDT as an
343 antimicrobial strategy. However, further research is warranted in order to optimize treatment
344 parameters, including a comprehensive evaluation of the effects of different total light doses
345 and a wider range of fluence rates. Additionally, investigating the underlying mechanisms of
346 curcumin-mediated aPDT in these microorganisms, including the specific cellular targets
347 and the generation of ROS, will be crucial for developing more effective and targeted
348 antimicrobial therapies.

349

350 **Disclosure statement:** The authors report there are no competing interests to declare.

351

352 **Funding details:** This work was supported by the Alexander von Humboldt Foundation
353 (grant number COL-1224696-GF-P, to J.A.G.-D.).

354

References

Alvarez N, Sevilla A. 2024. Current Advances in Photodynamic Therapy (PDT) and the Future Potential of PDT-Combinatorial Cancer Therapies. Int. J. Mol. Sci. 25:1023. Epub 2024 Jan 13. eng. doi:10.3390/ijms25021023.

Andrade MC, Ribeiro APD, Dovigo LN, Brunetti IL, Giampaolo ET, Bagnato VS, Pavarina AC. 2013. Effect of different pre-irradiation times on curcumin-mediated photodynamic therapy against planktonic cultures and biofilms of Candida spp. Arch. Oral Biol. 58:200–210. Epub 2012 Nov 13. eng. doi:10.1016/j.archoralbio.2012.10.011.

Angell-Petersen E, Spetalen S, Madsen SJ, Sun C-H, Peng Q, Carper SW, Sioud M, Hirschberg H. 2006. Influence of light fluence rate on the effects of photodynamic therapy in an orthotopic rat glioma model. J. Neurosurg. 104:109–117. eng. doi:10.3171/jns.2006.104.1.109.

Annunzio SR de, Freitas LM de, Blanco AL, da Costa MM, Carmona-Vargas CC, Oliveira KT de, Fontana CR. 2018. Susceptibility of Enterococcus faecalis and Propionibacterium acnes to antimicrobial photodynamic therapy. J. Photochem. Photobiol., B. 178:545–550. Epub 2017 Dec 5. eng. doi:10.1016/j.jphotobiol.2017.11.035.

Ansel HC, Norred WP, Roth IL. 1969. Antimicrobial activity of dimethyl sulfoxide against Escherichia coli, Pseudomonas aeruginosa, and Bacillus megaterium. J. Pharm. Sci. 58:836–839. eng. doi:10.1002/jps.2600580708.

Bapat PS, Nobile CJ. 2021. Photodynamic Therapy Is Effective Against Candida auris Biofilms. Front. Cell Infect. Microbiol. 11:713092. Epub 2021 Sep 3. eng. doi:10.3389/fcimb.2021.713092.

Cieplik F, Deng D, Crielaard W, Buchalla W, Hellwig E, Al-Ahmad A, Maisch T. 2018. Antimicrobial photodynamic therapy - what we know and what we don't. Crit. Rev. Microbiol. 44:571–589. Epub 2018 May 11. eng. doi:10.1080/1040841X.2018.1467876.

Dias LD, Blanco KC, Mfouo-Tynga IS, Inada NM, Bagnato VS. 2020. Curcumin as a photosensitizer: From molecular structure to recent advances in antimicrobial photodynamic therapy. J. Photochem. Photobiol., C. 45:100384. doi:10.1016/j.jphotochemrev.2020.100384.

Dos Santos AF, Almeida DRQ de, Terra LF, Wailemann RAM, Gomes VM, Arini GS, Ravagnani FG, Baptista MS, Labriola L. 2020. Fluence Rate Determines PDT Efficiency in Breast Cancer Cells Displaying Different GSH Levels. Photochem Photobiol. 96:658–667. Epub 2019 Dec 17. eng. doi:10.1111/php.13182.

Dougherty TJ, Gomer CJ, Henderson BW, Jori G, Kessel D, Korbelik M, Moan J, Peng Q. 1998. Photodynamic therapy. J. Natl. Cancer Inst. 90:889–905. eng. doi:10.1093/jnci/90.12.889.

Dovigo LN, Pavarina AC, Carmello JC, Machado AL, Brunetti IL, Bagnato VS. 2011. Susceptibility of clinical isolates of Candida to photodynamic effects of curcumin. Lasers Surg. Med. 43:927–934. eng. doi:10.1002/lsm.21110.

Dovigo LN, Pavarina AC, Ribeiro APD, Brunetti IL, Costa CAdS, Jacomassi DP, Bagnato VS, Kurachi C. 2011. Investigation of the photodynamic effects of curcumin against Candida albicans. Photochem Photobiol. 87:895–903. Epub 2011 Jun 13. eng. doi:10.1111/j.1751-1097.2011.00937.x.

Du H, Bing J, Hu T, Ennis CL, Nobile CJ, Huang G. 2020. Candida auris: Epidemiology, biology, antifungal resistance, and virulence. PLoS Pathog. 16:e1008921. Epub 2020 Oct 22. eng. doi:10.1371/journal.ppat.1008921.

Free SJ. 2013. Fungal cell wall organization and biosynthesis. Adv. Genet. 81:33–82. eng. doi:10.1016/B978-0-12-407677-8.00002-6.

Gao R, Xu H, Liu L, Zhang Y, Yin T, Zhou H, Sun M, Chen N, Ren Y, Chen T, et al. 2020. Photoacoustic visualization of the fluence rate dependence of photodynamic therapy. Biomed. Opt. Express. 11:4203–4223. Epub 2020 Jul 10. eng. doi:10.1364/BOE.395562.

Gao Y, Wu J, Li Z, Zhang X, Lu N, Xue C, Leung AW, Xu C, Tang Q. 2019. Curcumin-mediated photodynamic inactivation (PDI) against DH5α contaminated in oysters and cellular toxicological evaluation of PDI-treated oysters. Photodiagnosis Photodyn. Ther. 26:244–251. Epub 2019 Apr 3. eng. doi:10.1016/j.pdpdt.2019.04.002.

Gershman MD, Kennedy DJ, Noble-Wang J, Kim C, Gullion J, Kacica M, Jensen B, Pascoe N, Saiman L, McHale J, et al. 2008. Multistate outbreak of Pseudomonas fluorescens bloodstream infection after exposure to contaminated heparinized saline flush prepared by a compounding pharmacy. Clin. Infect. Dis. 47:1372–1379. eng. doi:10.1086/592968.

Ghorbani J, Rahban D, Aghamiri S, Teymouri A, Bahador A. 2018. Photosensitizers in antibacterial photodynamic therapy: an overview. Laser Ther. 27:293–302. eng. doi:10.5978/islsm.27_18-RA-01.

Grizante Barião PH, Tonani L, Brancini GTP, Nascimento E, Braga GÚL, Wainwright M, Zeska Kress MR von. 2022. In vitro and in vivo photodynamic efficacies of novel and conventional phenothiazinium photosensitizers against multidrug-resistant Candida auris. Photochem. Photobiol. Sci. 21:1807–1818. Epub 2022 Jul 11. eng. doi:10.1007/s43630-022-00258-4.

Grossman CE, Carter SL, Czupryna J, Le Wang, Putt ME, Busch TM. 2016. Fluence Rate Differences in Photodynamic Therapy Efficacy and Activation of Epidermal Growth Factor Receptor after Treatment of the Tumor-Involved Murine Thoracic Cavity. Int. J. Mol. Sci. 17:101. Epub 2016 Jan 14. eng. doi:10.3390/ijms17010101.

Henderson BW, Busch TM, Snyder JW. 2006. Fluence rate as a modulator of PDT mechanisms. Lasers Surg. Med. 38:489–493. eng. doi:10.1002/lsm.20327.

428 Hu P, Huang P, Chen MW. 2013. Curcumin reduces Streptococcus mutans biofilm
429 formation by inhibiting sortase A activity. Arch. Oral Biol. 58:1343–1348. Epub 2013 Jun
430 16. eng. doi:10.1016/j.archoralbio.2013.05.004.
431 Huis In 't Veld RV, Heuts J, Ma S, Cruz LJ, Ossendorp FA, Jager MJ. 2023. Current Challenges
432 and Opportunities of Photodynamic Therapy against Cancer. Pharmaceutics. 15:330.
433 Epub 2023 Jan 18. eng. doi:10.3390/pharmaceutics15020330.
434 Jao Y, Ding S-J, Chen C-C. 2023. Antimicrobial photodynamic therapy for the treatment of
435 oral infections: A systematic review. J. Dent. Sci. 18:1453–1466. Epub 2023 Jul 11. eng.
436 doi:10.1016/j.jds.2023.07.002.
437 Jori G, Fabris C, Soncin M, Ferro S, Coppellotti O, Dei D, Fantetti L, Chiti G, Roncucci G.
438 2006. Photodynamic therapy in the treatment of microbial infections: basic principles
439 and perspective applications. Lasers Surg. Med. 38:468–481. eng.
440 doi:10.1002/lsm.20361.
441 Kaur S, Modi NH, Panda D, Roy N. 2010. Probing the binding site of curcumin in Escherichia
442 coli and Bacillus subtilis FtsZ--a structural insight to unveil antibacterial activity of
443 curcumin. Eur. J. Med. Chem. 45:4209–4214. Epub 2010 Jun 22. eng.
444 doi:10.1016/j.ejmech.2010.06.015.
445 Klausen M, Ucuncu M, Bradley M. 2020. Design of Photosensitizing Agents for Targeted
446 Antimicrobial Photodynamic Therapy. Molecules. 25:5239. Epub 2020 Nov 10. eng.
447 doi:10.3390/molecules25225239.
448 Kumar H, Franzetti L, Kaushal A, Kumar D. 2019. Pseudomonas fluorescens: a potential
449 food spoiler and challenges and advances in its detection. Ann. Microbiol. 69:873–883.
450 doi:10.1007/s13213-019-01501-7.
451 Lan X, Liu Y, Wang L, Wang H, Hu Z, Dong H, Yu Z, Yuan Y. 2023. A review of curcumin in food
452 preservation: Delivery system and photosensitization. Food Chem. 424:136464. Epub
453 2023 May 26. eng. doi:10.1016/j.foodchem.2023.136464.
454 Law SK, Leung AWN, Xu C. 2023. Photodynamic Action of Curcumin and Methylene Blue
455 against Bacteria and SARS-CoV-2-A Review. Pharmaceuticals. 17:13. Epub 2023 Dec 25.
456 eng. doi:10.3390/ph17010034.
457 Laxminarayan R, Matsoso P, Pant S, Brower C, Røttingen J-A, Klugman K, Davies S. 2016.
458 Access to effective antimicrobials: a worldwide challenge. Lancet. 387:168–175. Epub
459 2015 Nov 18. eng. doi:10.1016/S0140-6736(15)00474-2.
460 Liu J, Zhang H, Zhang L, Li T, Liu N, Liu Q. 2023. Effect of various concentrations of common
461 organic solvents on the growth and proliferation ability of Candida glabrata and their
462 permissible limits for addition in drug susceptibility testing. PeerJ. 11:e16444. Epub
463 2023 Nov 21. eng. doi:10.7717/peerj.16444.

464 Liu X, Xiang L, Yin Y, Li H, Ma D, Qu Y. 2021. Pneumonia caused by Pseudomonas
465 fluorescens: a case report. BMC Pulm. Med. 21:212. Epub 2021 Jul 5. eng.
466 doi:10.1186/s12890-021-01573-9.
467 Nataro JP, Kaper JB. 1998. Diarrheagenic Escherichia coli. Clin. Microbiol. Rev. 11:142–201.
468 eng. doi:10.1128/CMR.11.1.142.
469 Nichols MG, Foster TH. 1994. Oxygen diffusion and reaction kinetics in the photodynamic
470 therapy of multicell tumour spheroids. Phys. Med. Biol. 39:2161–2181. eng.
471 doi:10.1088/0031-9155/39/12/003.
472 Oliveira EF de, Tosati JV, Tikekar RV, Monteiro AR, Nitin N. 2018. Antimicrobial activity of
473 curcumin in combination with light against Escherichia coli O157:H7 and Listeria
474 innocua: Applications for fresh produce sanitation. Postharvest Biol. Biotechnol.
475 137:86–94. doi:10.1016/j.postharvbio.2017.11.014.
476 Penha CB, Bonin E, da Silva AF, Hioka N, Zanqueta ÉB, Nakamura TU, Abreu Filho BA de,
477 Campanerut-Sá PAZ, Mikcha JMG. 2017. Photodynamic inactivation of foodborne and
478 food spoilage bacteria by curcumin. LWT. 76:198–202. doi:10.1016/j.lwt.2016.07.037.
479 Polat E, Kang K. 2021. Natural Photosensitizers in Antimicrobial Photodynamic Therapy.
480 Biomedicines. 9:584. Epub 2021 May 21. eng. doi:10.3390/biomedicines9060584.
481 Praditya D, Kirchhoff L, Brüning J, Rachmawati H, Steinmann J, Steinmann E. 2019. Anti-
482 infective Properties of the Golden Spice Curcumin. Front. Microbiol. 10:912. Epub 2019
483 May 3. eng. doi:10.3389/fmicb.2019.00912.
484 Prates RA, Silva EG, Yamada AM, Suzuki LC, Paula CR, Ribeiro MS. 2009. Light parameters
485 influence cell viability in antifungal photodynamic therapy in a fluence and rate fluence-
486 dependent manner. Laser Phys. 19:1038–1044. doi:10.1134/S1054660X09050284.
487 Priyadarsini KI. 2009. Photophysics, photochemistry and photobiology of curcumin: Studies
488 from organic solutions, bio-mimetics and living cells. J. Photochem. Photobiol., C.
489 10:81–95. doi:10.1016/j.jphotochemrev.2009.05.001.
490 Qin Y, Luan X, Bi L, He G, Bai X, Zhou C, Zhang Z. 2008. Toluidine blue-mediated
491 photoinactivation of periodontal pathogens from supragingival plaques. Lasers Med.
492 Sci. 23:49–54. Epub 2007 Mar 15. eng. doi:10.1007/s10103-007-0454-x.
493 Rangel JM, Sparling PH, Crowe C, Griffin PM, Swerdlow DL. 2005. Epidemiology of
494 Escherichia coli O157:H7 outbreaks, United States, 1982-2002. Emerg. Infect. Dis.
495 11:603–609. eng. doi:10.3201/eid1104.040739.
496 Santezi C, Reina BD, Dovigo LN. 2018. Curcumin-mediated Photodynamic Therapy for the
497 treatment of oral infections-A review. Photodiagnosis Photodyn. Ther. 21:409–415. Epub
498 2018 Feb 22. eng. doi:10.1016/j.pdpdt.2018.01.016.
499 Saraiva BB, Campanholi KdSS, Machado RRB, Nakamura CV, Silva AA, Caetano W, Pozza
500 MSdS. 2024. Reducing Pseudomonas fluorescens in milk through photodynamic

inactivation using riboflavin and curcumin with 450 nm blue light-emitting diode. Int. Dairy J. 148:105787. doi:10.1016/j.idairyj.2023.105787.

Saraiva BB, Rodrigues BM, da Silva Junior RC, Scapim MRdS, Lancheros CAC, Nakamura CV, Caetano W, Pereira PCdS, Santana EHW de, Pozza MSdS. 2021. Photodynamic inactivation of Pseudomonas fluorescens in Minas Frescal cheese using curcumin as a photosensitizer. LWT. 151:112143. doi:10.1016/j.lwt.2021.112143.

Silva AR, Cabral FV, Silva CR, Silva DFT, Freitas AZ, Fontes A, Ribeiro MS. 2023. New Insights in Phenothiazinium-Mediated Photodynamic Inactivation of Candida Auris. J. Fungi. 9:717. Epub 2023 Jun 30. eng. doi:10.3390/jof9070717.

Sitnik TM, Henderson BW. 1998. The Effect of Fluence Rate on Tumor and Normal Tissue Responses to Photodynamic Therapy. Photochem Photobiol. 67:462–466. doi:10.1111/j.1751-1097.1998.tb05228.x.

Tunçer Çağlayan S, Gurbanov R. 2024. Modulation of bacterial membranes and cellular macromolecules by dimethyl sulfoxide: A dose-dependent study providing novel insights. Int. J. Biol. Macromol. 267:131581. Epub 2024 Apr 12. eng. doi:10.1016/j.ijbiomac.2024.131581.

Wainwright M. 1998. Photodynamic antimicrobial chemotherapy (PACT). J. Antimicrob. Chemother. 42:13–28. eng. doi:10.1093/jac/42.1.13.

Wang H-W, Rickter E, Yuan M, Wileyto EP, Glatstein E, Yodh A, Busch TM. 2007. Effect of photosensitizer dose on fluence rate responses to photodynamic therapy. Photochem Photobiol. 83:1040–1048. eng. doi:10.1111/j.1751-1097.2007.00139.x.

Woodhams JH, Macrobert AJ, Bown SG. 2007. The role of oxygen monitoring during photodynamic therapy and its potential for treatment dosimetry. Photochem. Photobiol. Sci. 6:1246–1256. Epub 2007 Sep 21. eng. doi:10.1039/b709644e.

Xie L, Ji X, Zhang Q, Wei Y. 2022. Curcumin combined with photodynamic therapy, promising therapies for the treatment of cancer. Biomed. Pharmacother. 146:112567. Epub 2021 Dec 22. eng. doi:10.1016/j.biopha.2021.112567.

Yamamoto J, Yamamoto S, Hirano T, Li S, Koide M, Kohno E, Okada M, Inenaga C, Tokuyama T, Yokota N, et al. 2006. Monitoring of singlet oxygen is useful for predicting the photodynamic effects in the treatment for experimental glioma. Clin. Cancer Res. 12:7132–7139. eng. doi:10.1158/1078-0432.CCR-06-0786.

Youf R, Müller M, Balasini A, Thétiot F, Müller M, Hascoët A, Jonas U, Schönherr H, Lemercier G, Montier T, et al. 2021. Antimicrobial Photodynamic Therapy: Latest Developments with a Focus on Combinatory Strategies. Pharmaceutics. 13:1995. Epub 2021 Nov 24. eng. doi:10.3390/pharmaceutics13121995.

Yu X, Zou Y, Zhang Z, Wei T, Ye Z, Yuk H-G, Zheng Q. 2022. Recent advances in antimicrobial applications of curcumin-mediated photodynamic inactivation in foods. Food Control. 138:108986. doi:10.1016/j.foodcont.2022.108986.

539 Zheng S, Yan H, Deng P, Zhu J, Lu H. 2025. Enhancement of curcumin-mediated
540 photodynamic inactivation against Pseudomonas fluorescens on fish fillets combined
541 with ε-polylysine hydrochloride. LWT:117344. doi:10.1016/j.lwt.2025.117344.
542